BIOCHEMISTRY
including biophysical chemistry & molecular biology

Article

pubs.acs.org/biochemistry

Intramolecular Interactions within the Human Immunodeficiency Virus-1 gp41 Loop Region and Their Involvement in Lipid Merging

Avraham Ashkenazi, Elisa Merklinger,[†] and Yechiel Shai*

Department of Biological Chemistry, The Weizmann Institute of Science, Rehovot, 76100 Israel

ABSTRACT: The human immunodeficiency virus utilizes its gp41 fusion protein to mediate virus−cell membrane fusion. The conserved disulfide loop region in the gp41 hairpin conformation reverses the protein chain, such that the N-terminal heptad repeat and the C-terminal heptad repeat regions interact to form the six-helix bundle. Hence, it is conceivable that the sequential folded N- and C-terminal parts of the loop region also interact. We show that the N- and C-terminal parts of the loop preferably form disulfide-bonded heterodimers with slow oxidation kinetics. Furthermore, when the two parts were linked to a single polypeptide to form the full-length loop, only an intramolecular disulfide-bonded loop was formed. Fluorescence studies revealed that an interaction takes place between the N- and C-terminal parts of the loop in solution, which was sustained in membranes. Functionally, only a combination of the N- and C-loop parts induced lipid mixing of model liposomes, the level of which increased 8-fold when they were connected to a single polypeptide chain. In both cases, the activity was independent of the oxidation state of the cysteines. Overall, the data (i) provide evidence of a specific interaction between the N- and C-terminal parts of the loop, which can further stabilize gp41 hairpin conformation, and (ii) suggest that the interaction between the N- and C-terminal parts of the loop is sufficient to induce lipid merging without forming a disulfide bond.

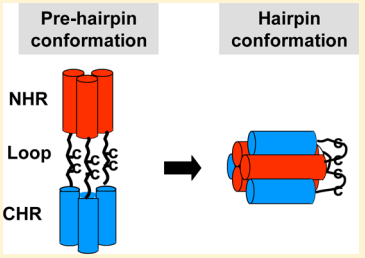

Membrane fusion is a fundamental step needed for the entry of the human immunodeficiency virus (HIV) into host cells.[1] The fusion step is mediated by the viral envelope protein (ENV) organized as a trimer; each monomer consists of two noncovalently associated subunits, gp120 and gp41.[2,3] gp120 mediates binding to cellular receptors and coreceptors, whereas gp41 is responsible for the actual membrane fusion event.[4,5]

During fusion, the HIV ENV exists in at least three conformations. (i) Initially, the ENV is in a metastable native conformation, in which gp41 is thought to be sheltered by gp120.[5] (ii) The binding of gp120 to cell receptors involves conformational changes in both subunits, resulting in a prehairpin conformation in which gp41 is exposed and extended,[5−7] leading to insertion of the fusion peptide (FP) into the host cell membrane.[8−10] At this stage, the N-terminal heptad repeat (NHR) and the C-terminal heptad repeat (CHR) regions are not associated. (iii) Subsequently, a trimeric central NHR coiled coil is packed by the three CHR regions in an antiparallel manner (illustrated in Figure 1A) to form the folded hairpin conformation. This structure is often termed the six-helix bundle (SHB) or "core" structure.[11,12] Folding of the NHR and CHR regions into the SHB is vital for maintaining and expanding the membrane fusion pore.[13,14]

It has already been demonstrated that the SHB structure in the dynamic fusion reaction is larger than that analyzed using the crystal structure (based on N36 and C34 peptides that are derived from the NHR and CHR regions, respectively).[15−17] Moreover, other N- and C-terminal regions outside the central SHB also participate in stabilizing the gp41 hairpin conformation, thereby assisting the membrane fusion reaction. Examples include (i) the N-terminal FP interaction with the C-terminal transmembrane domain (TMD), which induces fusion,[18] and (ii) the FP and TMD proximal external regions, which associate to further stabilize the gp41 hairpin conformation.[19,20]

The NHR and CHR regions are connected by the loop region, which reverses the protein chain.[21] The loop is structurally conserved in lentiviruses and contains two cysteines at the center of the region along with the N- and C-flanking parts.[22,23] Currently, no available structures of the HIV gp41 loop exist in solution or in the membrane. During the folding of gp41 into the hairpin conformation, the N- and C-flanking parts of the gp41 loop fold, too, and therefore are in the proximity of each other (illustrated in Figure 1A). Considering the model by which the NHR and the CHR regions of gp41 interact to stabilize the hairpin conformation, it is conceivable that the sequential folded N- and C-parts of the loop region also interact.

In this study, we synthesized the full-length gp41 loop region comprising the two cysteines and the N- and C-flanking parts of the loop, each consisting of one cysteine. We demonstrated that the N- and C-terminal parts of the loop interact in solution and in membranes. Functionally, the N- and C-terminal parts of the loop synergistically contribute to lipid merging regardless of the formation of a disulfide bond between them. Overall, the data shed light on the possible function of the conserved loop region during the conformational changes of the gp41 fusion protein of HIV.

Received: June 28, 2012
Revised: August 15, 2012
Published: August 16, 2012

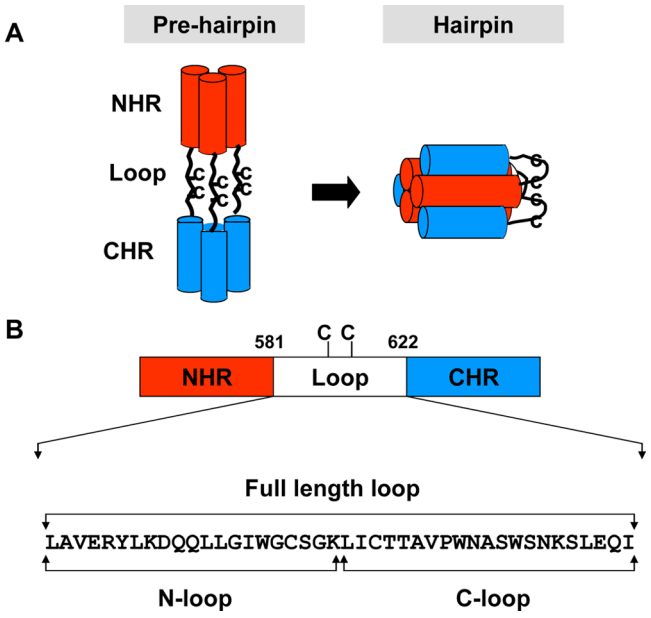

Figure 1. (A) Illustration of the accepted model for organizing the NHR, CHR, and loop regions in the gp41 prehairpin and hairpin conformations. In the prehairpin conformation, the gp41 trimer is extended. In the hairpin conformation, the trimeric central NHR coiled coil is packed by the three CHR regions in an antiparallel manner. The NHR and CHR regions are connected by the loop region, which reverses the protein chain and contains two cysteines in the center of the region. Consequently, the N- and C-flanking domains of the loop are in the proximity of each other. To simplify this illustration, only the NHR, CHR, and loop regions of gp41 are presented, and only one trimer is shown. (B) Designation and sequence of the full-length loop, the N-terminal domain of the loop (N-loop), and the C-terminal domain of the loop (C-loop). Each of the terminal domains contains one cysteine residue. Residue numbers correspond to gp160 of HIV-1 HXB2.

EXPERIMENTAL PROCEDURES

Materials. Fmoc amino acids, including lysine with an MTT side chain-protecting group and Fmoc rink amide MBHA resin, were purchased from Novabiochem AG (Laufelfinger, Switzerland). Tris(2-carboxyethyl)phosphine hydrochloride (TCEP), ethanedithiol (EDT), phosphatidylcholine (PC) from egg yolk, cholesterol (Chol), egg yolk sphingomyelin (SM), L-α-phosphatidylethanolamine (PE) from egg yolk, and L-α-lysophosphatidylcholine were purchased from Sigma Chemical Co. Rho [5(6)-carboxytetramethylrhodamine *N*-succinimidyl ester] was obtained from Biotium. *N*-(Lissamine rhodamine B sulfonyl) dioleoylphosphatidylethanolamine (Rho-PE) and *N*-(7-nitrobenz-2-oxa-1,3-diazol-4-yl)-dioleoylphosphatidylethanolamine (NBD-PE) were purchased from Molecular Probes (Eugene, OR).

Peptide Synthesis and Fluorescent Labeling. Peptides were synthesized with an automatic peptide synthesizer (433A from Applied Biosystems) on rink amide MBHA resin by using the Fmoc strategy as previously described.[24] Peptides with cysteine residues were cleaved with a TFA/DDW/TES/thioanisole/EDT [92.1:3.9:1.25:1.25:2.5 (v/v)] mixture. Before reverse phase high-performance liquid chromatography (RP-HPLC) purification to >95%, the samples were dissolved in 5 mM TCEP as a reducing agent, and the peptides were purified under acidic conditions with 0.1% (v/v) TFA to maintain the cysteine residues in a reduced form. The rhodamine (emission at 580 nm; excitation at 530 nm) fluorescent probe was coupled to the N-terminus of selected peptides in DMF with 2% DIEA overnight. The molecular weight of the peptides was confirmed by platform LCA electrospray mass spectrometry.

Kinetics of Oxidation of the Loop and Dimerization of the N- and C-Loop Parts. The purified N- and C-loop peptides were maintained as powders and were dissolved (1:1 molar ratio) just before the experiments started (a total of 100 μg/mL) in PBS (pH 7.4) without magnesium or calcium. To verify the formation of disulfide bonds, the loop peptides were first dissolved in PBS supplemented with a reducing agent, TCEP (1−5 mM). Oxidation was performed under stirring conditions, and the peptides were exposed to air for 24 h. Samples were subjected to RP-HPLC to monitor the oxidation process and the formation of dimers. The peptides were eluted at a flow rate of 0.6 mL/min over 40 min using a linear gradient from 25:75 (v/v) to 55:45 (v/v) CH_3CN/H_2O on an analytical C4 column (5 μm particle size, 0.46 cm × 25 cm) from GraceVydac. The retention times of the oxidized peptides were as follows: 23.9 min for the C homodimer, 24.3 min for the NC heterodimer, and 24.7 min for the N homodimer. To calculate the ratio between the dimers, the amount of heterodimer was divided by the sum of the amount of both homodimers.

The oxidation of the full-length loop was also performed as described above. The full-length loop peptides were eluted at a flow rate of 0.6 mL/min using a linear gradient from 25:75 (v/v) to 45:55 (v/v) CH_3CN/H_2O over 40 min and from 45:55 (v/v) to 80:20 (v/v) CH_3CN/H_2O over 10 min. An analytical C4 column (5 μm particle size, 0.46 cm × 25 cm) from GraceVydac was used. The retention times were 27.2 and 25.8 min for the reduced loop and oxidized loop, respectively.

Preparation of LUVs. Thin films were generated following dissolution of the lipids in a 2:1 (v/v) chloroform/methanol mixture and then dried under a stream of nitrogen gas while they were rotated. Two populations of films were generated: (i) unlabeled, containing 1:1:1:1 PC/SM/PE/Chol LUVs, and (ii) labeled, containing a 1:1:1:1 PC/SM/PE/Chol mixture and 0.6 mol % NBD-PE and Rho-PE each. The films were lyophilized overnight, and the containers were sealed with argon gas to prevent oxidation and stored at −20 °C. Before an experiment, the films were suspended in PBS and vortexed for 1.5 min. The lipid suspension underwent five cycles of freezing and thawing followed by extrusion through polycarbonate membranes with 1 and 0.1 μm diameter pores 21 times to create large unilamellar vesicles (LUVs).

Analysis of Interactions Utilizing Competition Experiments with Fluorescently Labeled Peptides. Fluorescence quenching of the rhodamine probe was measured at room temperature using a SLM-AMINCO Bowman series 2 luminescence spectrometer as previously described.[25] The emission of rhodamine was monitored at 580 nm with the excitation set at 530 nm. Typical spectral bandwidths were 8 nm for excitation and 8 nm for emission. The sample was placed in 5 mm × 5 mm quartz cuvettes with constant magnetic stirring. The rhodamine-labeled peptides were dissolved in either 400 μL of HEPES (5 mM, pH 7.4) or 100 μM LUVs in HEPES. To examine the peptides' interaction, competition experiments were performed. The fluorescence of rhodamine-labeled C-loop peptides (0.5 μM) was measured alone or with a 5-fold molar excess of unlabeled N- or C-loop peptides. All fluorescence measurements were recorded before and after the addition of proteinase K (final concentration of 125 ng/μL), to

dx.doi.org/10.1021/bi300868f | *Biochemistry* 2012, 51, 6981−6989

follow the kinetics of enzymatic peptide degradation and recovery of the fluorescent signal.

Lipid Mixing Assay. Lipid mixing of LUVs was measured using a fluorescence probe dilution assay.[26] LUVs were prepared with PBS, as described above, from unlabeled and labeled films combined to yield a 9:1 ratio with a final lipid concentration of 100 μM. The basal fluorescence level was measured initially for a 400 μL vesicle mixture. Then, C- or N-loop peptides, dissolved in 2 μL of DMSO, were added to the mixture alone or together at 1:1 molar ratio (half the respective concentrations of the single peptides to give the same total peptide concentration). The fluorescence was monitored for a maximum of 15 min after the peptide was added, to ensure a steady state, as indicated by a plateau. When labeled vesicles are fused with unlabeled vesicles to form a new membrane, this results in a reduced surface density of the rhodamine energy acceptor. Consequently, lipid mixing reduces the efficiency of the resonance energy transfer, which is measured by the increase in the fluorescence of the NBD serving as an energy donor. In some experiments, the peptides were preincubated with 1 mM TCEP before being added to the lipid mixture. The emission of NBD was monitored at 530 nm with the excitation set at 467 nm. The fluorescence intensity before the addition of peptide was termed 0% lipid mixing. A 100% lipid mixing was normalized according to 2% (v/v) Triton xs-100. Additionally, the rates of lipid mixing were also calculated and expressed as the *x*-fold increase in NBD fluorescence after the addition of the peptides.

Visible Absorbance Measurements. Changes in the size of the vesicles were measured by using visible absorbance. Aliquots of peptide stock solutions were added to suspensions of LUVs in PBS at a final lipid concentration of 100 μM. The absorbance at 405 nm was monitored with time using a microplate reader before and after the addition of a peptide.

Electron Microscopy (EM). The effects of the peptides on liposome suspensions were determined by negative stain EM. Prior to staining and fixing, suspensions of PC/SM/PE/Chol (1:1:1:1) LUVs at 5 mM (with or without peptides) were incubated for 5 min at room temperature. A drop of the suspension containing LUVs or a mixture of LUVs and peptides at a peptide:lipid molar ratio of 0.1 was deposited onto a carbon-coated grid and negatively stained with 1% uranyl acetate. The grids were examined using a JEOL JEM 100B electron microscope (Japan Electron Optics Laboratory Co., Tokyo, Japan).

Secondary Structure Determination Utilizing Circular Dichroism (CD) Spectroscopy. CD measurements were performed by using an Applied Photophysics spectropolarimeter. The spectra were scanned using a thermostatic quartz cuvette with a path length of 1 mm. Wavelength scans were performed at 25 °C; the average recording time was 15 s, in 1 nm steps, in the wavelength range of 190−260 nm. Peptides were scanned at a concentration of 10 μM in solution (5 mM HEPES, pH 7.4) and in a membrane mimetic environment of 1% LPC in a HEPES solution.

RESULTS

Oxidation of the Cysteines Reveals a Preference for N- and C-Loop Heterodimers and Intramolecular Disulfide Bonds within the Full-Length Loop. The gp41 loop comprises two cysteines at the center of this region. The folding of gp41 to the SHB also leads to the folding of the loop. Here, to investigate possible interactions within the loop, we

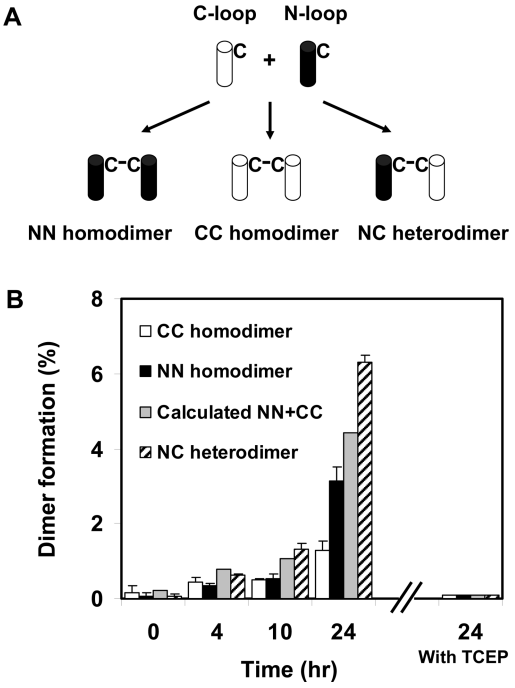

Figure 2. Disulfide-mediated dimerization of the N- and C-terminal loop parts. Purified N- and C-loop peptides were solubilized (1:1 molar ratio) at a final concentration of 100 μg/mL in PBS (pH 7.4). Peptides were allowed to form disulfide bonds at room temperature under stirring and were exposed to air for 24 h. The kinetics of dimer formation was monitored by RP-HPLC as described in Experimental Procedures. (A) Different possibilities of forming dimers in the oxidation system. (B) Percentages of CC homodimers, NN homodimers, and NC heterodimers in the oxidation system during the time of oxidation. The calculated sum of the two homodimers is also presented. In several experiments, the reducing agent, TCEP (1 mM), was also added to the oxidation system and the percentages of dimers were analyzed. Results represent the average ± SD.

divided the loop into the C- and N-terminal domains and separated the two cysteines (Figure 1B). The C-loop domain (with one cysteine) represents the C-terminal part of the loop, whereas the N-loop domain (with one cysteine) represents the N-terminal part of the region. The two parts were mixed together at a 1:1 molar ratio in PBS, and the oxidation kinetics of the peptides was followed by RP-HPLC. Three oxidative products were expected: NN homodimer, CC homodimer, and NC heterodimer (Figure 2A). The oxidation kinetics was slow (hours) and yielded preferably NC heterodimers (Figure 2B). This preference became stronger with time. To further probe dimer formation, a reducing agent (TCEP) was added to the reaction mixture. The formation of dimers was abolished following this addition (Figure 2B). The probability of these interactions occurring was determined by calculating the ratio between the amount of heterodimers and the amount of the two homodimers during the oxidation process [R = NC/(NN + CC)]. Assuming that the interactions between the peptides are random, the ratio should yield an R value of 1. Values that exceed 1 indicate that specific interactions favoring the formation of a heterodimer occur. Indeed, after 10 h, the calculated R value was 1.26, and after 24 h, the R value was 1.54. This suggests a significant preference for the formation of NC heterodimers.

The N- and C-loop parts were placed closer together by linking them to a single molecule of the full-length loop (Figure

dx.doi.org/10.1021/bi300868f | *Biochemistry* 2012, 51, 6981−6989

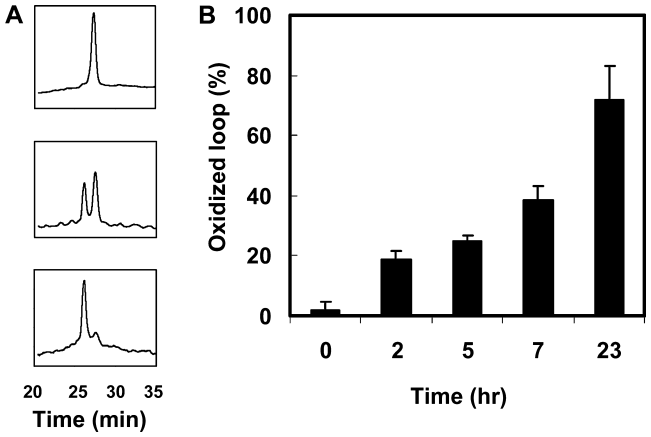

Figure 3. Analysis of disulfide bond formation within the full-length loop region. The purified full-length loop, with reduced cysteine residues, was oxidized as described for the dimerization assay. The kinetics of the different oxidative products that were formed was monitored by RP-HPLC. (A) HPLC chromatogram of the oxidative products. Intramolecular disulfide-bonded loop peptides were detected and eluted 1.4 min before the reduced loop peptides. The top panel shows the profile of a sample that was injected immediately after the oxidation started (t = 0). The middle panel shows the profile after oxidation for 7 h, and the bottom panel shows the profile after oxidation for 23 h. (B) Percentage of disulfide-bonded loop peptides in the oxidation system during the oxidation time. Results represent the average ± SD of the experiments.

1B). Oxidation of the loop was conducted in a manner similar to the oxidation process of the two loop parts, and the analysis of the oxidative products was performed by RP-HPLC. Because the loop contains two cysteines that were initially in a reduced form, one would expect a mixture of the following oxidative products: a dimer, an intramolecular disulfide-bonded loop, and a multimer chain. Importantly, only an intramolecular disulfide-bonded loop was detected, which was eluted 1.4 min before the reduced loop (Figure 3A). Oxidation of the full-length loop was much faster than that of the dimerization of the N- and C-loop parts, and 72% of the loop peptides were converted into disulfide-bonded loop peptides after 23 h (Figure 3B). Overall, the loop oxidation experiments revealed a significant preference for specific oxidation products that result from an interaction between the N- and C-terminal loop parts.

Fluorescence Studies Support an Interaction between the N- and C-Loop Parts That Are Sustained in the Membrane. Rhodamine fluorescence is self-quenched when the probes are in the proximity of each other. Thus, labeling peptides with rhodamine allows us to examine peptide−peptide interactions in solution and in membranes by monitoring the changes in rhodamine fluorescence. To analyze peptide interactions, we employed a competition strategy. Briefly, C-loop peptides were labeled with rhodamine, and their fluorescent signals were measured alone and in the presence of a 5-fold molar excess of unlabeled peptides. Figure 4A shows the fluorescence studies that were conducted in solution. Labeled C-loop peptides alone had high initial fluorescence. When the unlabeled counterpart N-loop peptides were added, the magnitude of the signal of the labeled C-loop peptides decreased. We reasoned that the N- and C-loop parts interacted in solution, which resulted in greater proximity of the rhodmaine-labeled C-loop peptides. This allowed their fluorescent signal to be quenched. As a control, only a small change was observed in the fluorescence of the labeled C-loop peptides when unlabeled C-loop peptides were introduced. Addition of proteinase K resulted in partial peptide degradation, which slowly dequenched the fluorescent signal, most probably because of the partial dissociation of the complex.

Next, to investigate whether this interaction is also sustained in membranes, the same experiment was performed in the presence of liposomes (Figure 4B). The loop region assembles in the membrane.[27] Indeed, the labeled C-loop peptides alone exhibited a relatively low initial fluorescent signal compared with that observed in solution, suggesting that they partially

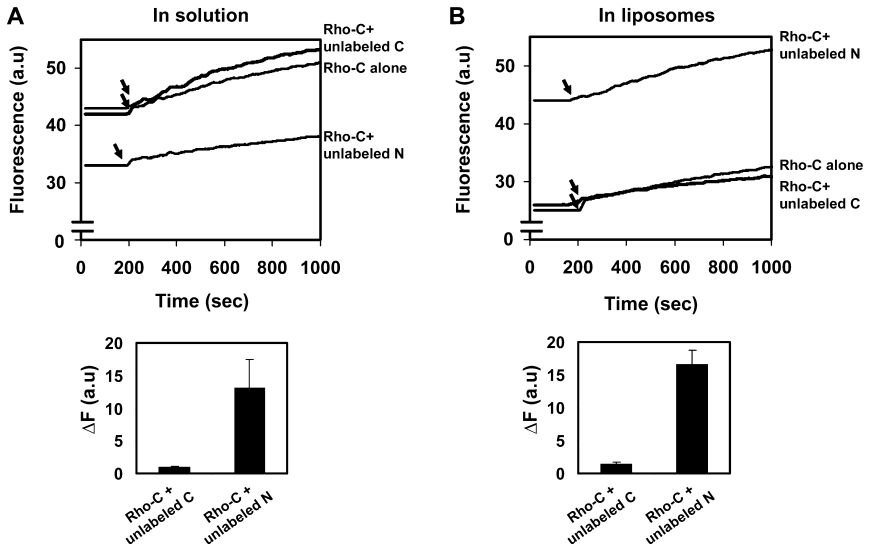

Figure 4. Competition assay utilizing fluorescently labeled loop peptides. The fluorescence of rhodamine-labeled C-loop peptides was monitored alone and in the presence of a 5-fold molar excess of unlabeled N- or C-loop peptides. Next, proteinase K (125 ng/μL) was added (denoted by an arrow). (A) Representative panel of fluorescence measurements in solution (5 mM HEPES, pH 7.4). (B) Representative panel of fluorescence measurements in liposomes containing 100 μM LUVs. The results of each panel were quantified and presented (in absolute values) as the means of changes in fluorescence (ΔF) in arbitrary units (a.u) ± SD.

dx.doi.org/10.1021/bi300868f | *Biochemistry* 2012, 51, 6981−6989

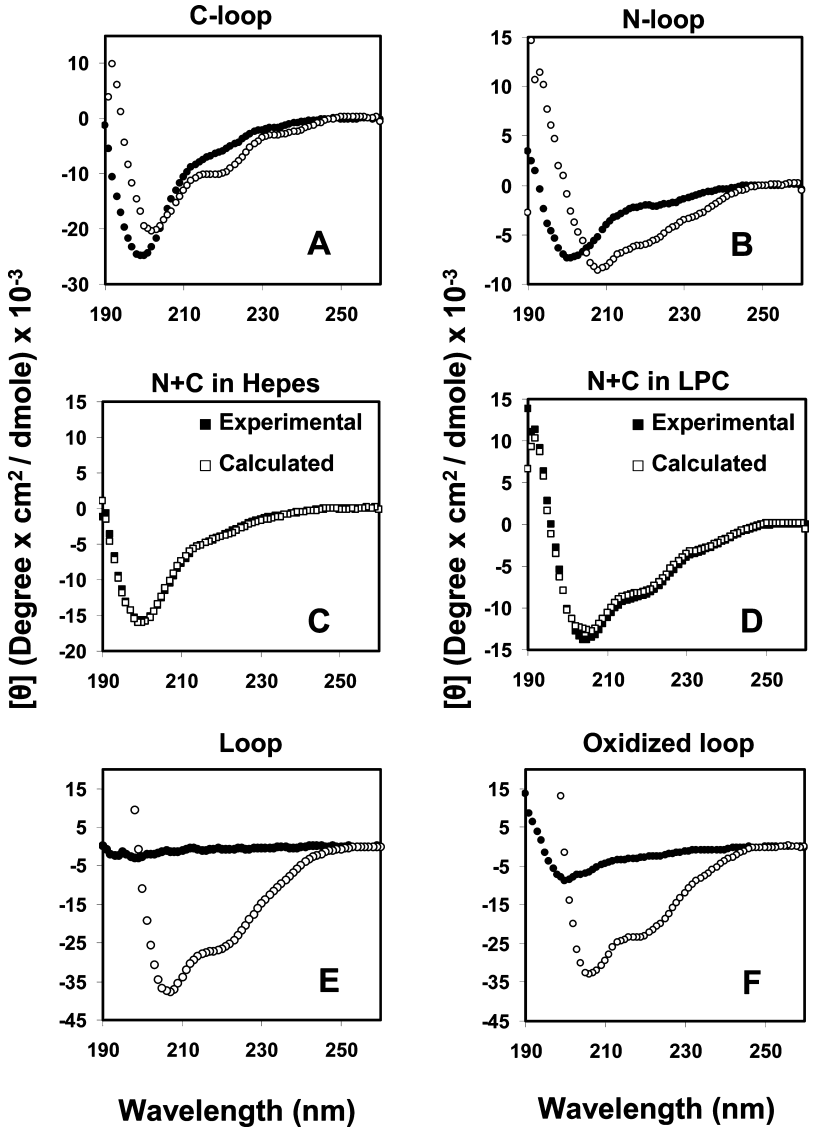

Figure 5. Secondary structure of the loop region and its N- and C-terminal parts utilizing CD spectroscopy. In panels A and B, the following peptides were scanned at a concentration of 10 μM in solution (5 mM HEPES, pH 7.4) (●) and in a membrane mimetic environment of 1% LPC in HEPES (○): (A) the C-terminal part of the loop and (B) the N-terminal part of the loop. Panels C and D show the calculated combined signal of the N-loop and C-loop (□) and the experimental signal monitored upon co-incubation of the two peptides at a 1:1 molar ratio (■). Panel C shows the measurements in solution, and panel D shows the measurements in a membrane mimetic environment. In panels E and F, the following peptides were scanned at a concentration of 10 μM in solution (5 mM HEPES, pH 7.4) (●) and in a membrane mimetic environment of 1% LPC in HEPES (○): (E) the full-length loop and (F) the oxidized full-length loop.

assemble in membranes (Figure 4B). The addition of the unlabeled counterpart N-loop peptides resulted in an increase in the signal of the labeled C-loop peptides. This may suggest that in membranes, the interaction between the N- and C-loop peptides caused the labeled C-loop peptide to be displaced by an unlabeled N-loop peptide. Thus, the labeled C-loop peptides were separated from each other, which resulted in an increase in the magnitude of their fluorescent signal. With regard to a control, only a small change was observed in the fluorescence of the labeled C-loop peptides when unlabeled C-loop peptides were introduced. Hence, the competition experiments with fluorescently labeled loop peptides further support the existence of an interaction between the N- and C-loop terminal parts.

Secondary Structure of the Loop Region and its N- and C-Parts in Solution and in a Membrane Mimetic Environment. We further examined the possible increase in the helical content of the N- and C-loop peptides upon their co-incubation to determine whether this feature correlates with their interaction pattern. Utilizing CD, the signals of the C-part and the N-part alone were measured in a solution and in a membrane mimetic environment (Figure 5A,B). Then, the signal of the C-part was added to the signal of the N-part to yield the calculated combined signal. This signal was compared to the actual experimental signal monitored upon co-incubation of the two peptides (Figure 5C,D). In solution, combining the two loop parts did not yield a CD-detectable helical structure, but in a membrane mimetic environment, an α-helical structure was detected. No difference in the CD signal was observed between the calculated and experimental signals of the two peptides in solution and in the membrane, indicating that no conformational change is induced by the peptide−peptide

dx.doi.org/10.1021/bi300868f | *Biochemistry* 2012, 51, 6981−6989

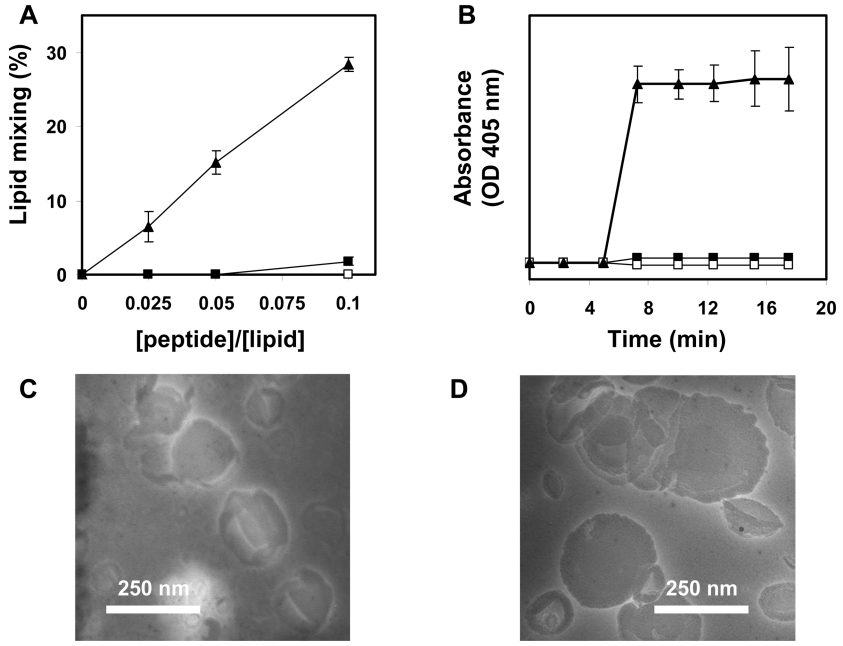

Figure 6. N- and C-terminal loop domains synergistically induce lipid mixing. (A) Dose-dependent lipid mixing of LUVs induced by the N-loop (■), the C-loop (□), and their combination in a premixed 1:1 molar ratio (▲). Peptide aliquots were added to 100 μM PC/SM/PE/Chol (1:1:1:1) LUVs in PBS, containing 10% prelabeled LUVs (0.6 mol % NBD-PE and Rho-PE) and 90% unlabeled LUVs. The increase in NBD fluorescence intensity was measured up to 15 min after the addition of the peptides. The percentage from the maximum [defined as the 2% (v/v) increase in fluorescence of Triton xs-100] was plotted vs the peptide:lipid molar ratio. (B) Lipid merging detection by a change in the absorbance of vesicles mixed with the peptide at 405 nm. The peptides were added to 100 μM LUVs in PBS. The changes in the absorbance are plotted vs the time after the addition of a peptide. Peptide designations are as follows: N-loop (■), C-loop (□), and their combination in a 1:1 molar ratio (▲). Bars indicate the SD of the experimental measurements. Panels C and D are electron micrographs of negatively stained 5 mM PC/SM/PE/Chol (1:1:1:1) LUVs in the absence and presence of N- and C-loop parts at a 0.1 peptide:lipid molar ratio. (C) LUVs alone. (D) LUVs with the loop peptides.

interactions. Moreover, the full-length loop and its oxidized analogue did not exhibit a detectable structure in solution (Figure 5E,F). Importantly, both forms of the loop adopted an α-helical structure to a similar extent in a membrane mimetic environment (Figure 5E,F).

The N- and C-Loop Parts Synergistically Induce Lipid Merging. The observations that the N- and C-loop parts could interact suggest that they play a functional role in the lipid merging process. We examined the ability of the N-loop, the C-loop, and a molar ratio of a 1:1 combination to induce lipid mixing of LUVs. Figure 6A shows that neither the N-loop nor the C-loop alone induced lipid mixing of LUVs up to a 0.1 peptide:lipid molar concentration ratio. Strikingly, their combination induced a significant dose-dependent vesicle merger. Membrane apposition is a necessary step before membrane fusion can occur. Changes in the vesicles' size distribution, resulting from aggregation and/or fusion, can be monitored by following the absorbance of liposome suspensions. The changes in the absorbance at 405 nm as a function of time at a peptide:lipid molar ratio of 0.1 are presented in Figure 6B. As in the lipid mixing assay, combining the N- and C-loop parts synergistically enhanced membrane apposition.

To confirm the lipid mixing activity of the loop, we compared the size of the vesicles alone or in the presence of the peptides by using EM. The EM images (Figure 6C,D) verified that adding the loop peptides induced marked vesicle enlargement compared with the untreated control image. The average size of the untreated vesicles was 123 ± 24 nm (n = 16), and the average size of the peptide-treated vesicles was 244 ± 80 nm (n = 14). $p < 0.001$.

The Interaction between the N- and C-Terminal Parts of the Loop Is Sufficient To Induce Lipid Merging without Forming a Disulfide Bond. The data revealed that the formation of disulfide bonds within the loop is slow (Figures 2 and 3). Thus, it is not reasonable that the formation of a disulfide bond between the N- and C-loop parts is essential for their lipid mixing activity, yet it is possible that the small portions of covalent dimers that were formed during the assay contributed to the lipid mixing activity. To investigate this possibility, we performed similar mixing experiments, but first the peptides were preincubated with a reducing agent. Furthermore, we analyzed the lipid mixing ability of the full-length loop and its oxidized analogue with an intramolecular disulfide bond. Figure 7A shows the rates of lipid mixing by calculating the x-fold increase in NBD fluorescence upon mixing induced by the different loop peptides. Clearly, the addition of a reducing agent did not change the ability of the N- and C-loop parts to synergistically induce lipid mixing. Increased lipid mixing activity was observed for the full-length loop, which was 8-fold higher than that resulting from combining the N- and C-loop parts. This was expected because the N- and C-loop parts are much closer when linked together into a single polypeptide chain. Importantly, the lipid mixing activity of the full-length loop was independent of the oxidation state of the cysteines. Another parameter that is involved in lipid mixing, besides detecting the rates of mixing, is the kinetics of the process. Figure 7B shows fast lipid mixing kinetics with a similar pattern when combining the N- and C-loop parts, the full-length loop, and the oxidized form of the loop. Thus, the data suggest that the interaction between the N-

dx.doi.org/10.1021/bi300868f | Biochemistry 2012, 51, 6981−6989

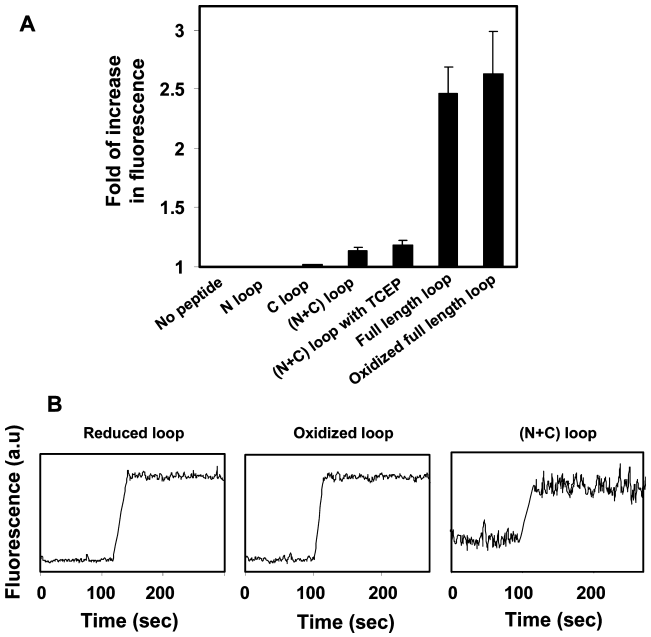

Figure 7. Rates and kinetics of lipid mixing induced by the loop domains with different oxidation states. (A) Peptides were added to PC/SM/PE/Chol (1:1:1:1) LUVs that contained unlabeled and labeled LUVs in a 9:1 molar ratio. Lipid mixing was monitored by measuring the increase in NBD fluorescence intensity. To compare the rates of lipid mixing between loop peptides with different oxidation states, the *x*-fold increase in NBD fluorescence was calculated after the addition of the peptides. Sometimes the peptides were preincubated with 1 mM TCEP. Bars indicate the SD of the experimental measurements. (B) Kinetics of the peptides' activity in the lipid mixing assay. The changes in fluorescence (arbitrary units) plotted vs time, after the addition of a peptide, are shown.

and C-terminal parts of the loop is sufficient to induce lipid mixing without forming a disulfide bond.

DISCUSSION

The HIV gp41 loop region is structurally conserved in lentiviruses and contains two cysteines at the center of the region along with N- and C-flanking domains.[21,22] Structurally, the loop connects the NHR and CHR regions and is thought to be extended in the gp41 prehairpin conformation. Then, the loop folds and reverses the gp41 protein chain, whereas the NHR and the CHR interact to form the SHB in the hairpin conformation.[28,29] It is well-known that the SHB is required for the membrane fusion process.[5,13,14] Additionally, it has been demonstrated that other N- and C-terminal regions of gp41 outside the SHB heteroassociate. Such interactions further stabilize the hairpin conformation, thereby contributing to fusion.[15,18,20] Importantly, we demonstrated an intramolecular interaction within the HIV gp41 loop region by its N- and C-terminal parts. Functionally, the interaction between the N- and C-parts of the loop synergistically induces lipid mixing that does not depend on the formation of disulfide bonds.

Association between the N- and C-Terminal Domains of the gp41 Loop. The interaction between the N- and C-terminal parts of the loop was analyzed using reporter systems of disulfide bond formation and fluorescence quenching. In both systems, a significant preference for the heterointeraction between the two parts was observed. No mutually induced folding of the two peptide fragments from the HIV gp41 loop region, however, was observed. Nevertheless, a structure exists in solution for the hairpin conformation of the simian immunodeficiency virus (SIV) comprising the loop region and the NHR and CHR regions, but lacking the cysteines.[23] This structure reveals that nonsequential intramolecular contacts exist between the two parts of the loop. Thus, the structure of the SIV loop further supports the occurrence of specific interactions between the flanking parts of the loop region. We showed that in solution there is no detectable α-helical structure for the loop. Moreover, the interaction between the N- and C-terminal parts of the loop is not accompanied by an increase in helical content (Figure 5). This can be explained by the formation of nonsequential contacts within the loop region of HIV gp41, like that observed in the loop structure of the SIV hairpin conformation. Consequently, it is conceivable that an association between the N- and C-terminal loop parts is required for forming a disulfide bond between them. This may also explain why only one oxidative product of the loop region was formed with an intramolecular disulfide bond.

Interestingly, portions of homodimers are also formed during the oxidation process, although to a lesser extent than the heterodimers. The number of N homodimers is much higher than the number of C homodimers (Figure 2B). The trimeric structure of the SIV hairpin conformation reveals intermolecular interactions between the loop regions, which are mediated by the N-part of the loop.[23] Considering the conservation of the loop within lentiviruses,[22] possible intermolecular interactions between the HIV gp41 N-loop parts could explain the formation of the N homodimers, as implied in Figure 2B.

Mechanism Underlying Lipid Merging Mediated by the Loop Region. Although the loop region is not a transmembrane segment, several lines of evidence indicate that this region has a membrane-active nature. The loop is one of the hydrophobic portions of gp41 and assembles in the membrane.[30,31] Interestingly, the region has no detectable helical structure in solution but adopts a strong α-helical structure in a membrane environment (Figure 5E,F). Moreover, the interaction between the N- and C-terminal parts of the loop is sustained in the membrane (Figure 4). Thus, it is conceivable that the loop region participates in the membrane fusion process. One of the contact sites between gp120 and gp41 resides in the loop region, where it triggers fusion activation.[28,29] Emerging studies show that the loop is involved in lipid mixing processes.[27,32−34] However, the contribution of the cysteines within the gp41 loop region in the actual membrane fusion step has been difficult to assess. This is because mutating them disrupts gp160 proteolytic processing,[35] and reducing agents that interfere with the thiol−disulfide interchange disrupt gp120−CD4 rearrangement.[36]

Thermodynamic studies suggest that the energy required to fuse two stable membrane bilayers is mainly dependent on the pore-opening step, which is the rate-limiting step. The lipid mixing step, however, is much faster.[37] Here we show that only the combination of the N- and C-terminal domains of the loop results in a significant lipid mixing effect. Taking into consideration the slow kinetics of formation of disulfide bonds, we find it is not reasonable that the lipid mixing ability of the N- and C-loop parts would mainly be dependent on the disulfide interaction between them. Indeed, rapid synergistic lipid mixing activity is observed between the N- and C-terminal parts of the loop, which is unaffected by adding a reducing

dx.doi.org/10.1021/bi300868f | *Biochemistry* 2012, 51, 6981−6989

agent. Moreover, the presence of an intramolecular disulfide bond within the full-length loop results in a lipid mixing rate similar to that of the reduced form (Figure 7). Thus, we suggest that lipid merging processes induced by the loop are initiated by an interaction between the N- and C-terminal domains of the loop, and not by the disulfide bonds formed between them. We believe that under intact conditions, when the N- and C-terminal domains of the loop are located within the full gp41 protein, disulfide bonds may be beneficial for further maintaining the interaction between the terminal-flanking parts of the loop during the membrane fusion reaction.

In summary, in this study we demonstrate that the N- and C-terminal domains of the HIV gp41 loop associate with each other. This association synergistically induces lipid merging. Hence, these data further support the model by which multiple regions within gp41 contribute to the stability of the hairpin conformation and assist in membrane fusion. Because the loop is structurally conserved in lentiviruses, the findings may also shed light on the function of the loop region during the fusion protein conformational changes of other viruses.

AUTHOR INFORMATION

Corresponding Author

*Department of Biological Chemistry, The Weizmann Institute of Science, Rehovot, 76100 Israel. Telephone: 972-8-9342711. Fax: 972-8-9344112. E-mail: yechiel.shai@weizmann.ac.il.

Present Address

[†]Membrane Biochemistry, Life and Medical Sciences (LIMES) Institute, University of Bonn, Bonn, Germany.

Funding

This study was supported by Israel Science Foundation Grant 988/09. Y.S. is the incumbent of the Harold S. and Harriet B. Brady Professorial Chair in Cancer Research.

Notes

The authors declare no competing financial interest.

ACKNOWLEDGMENTS

We thank Batya Zarmi for her valuable help with peptide purification and Yehuda Marikovsky for assisting in recording and analyzing the images in the electron microscope.

ABBREVIATIONS

Chol, cholesterol; CHR, C-terminal heptad repeat; CD, circular dichroism; EM, electron microscopy; ENV, viral envelope protein; FP, fusion peptide; HIV, human immunodeficiency virus; LUVs, large unilamellar vesicles; NHR, N-terminal heptad repeat; PC, phosphatidylcholine; PE, phosphatidylethanolamine; RP-HPLC, reverse phase high-performance liquid chromatography; SD, standard deviation; SIV, simian immunodeficiency virus; SM, sphingomyelin; SHB, six-helix bundle; TMD, transmembrane domain.

REFERENCES

(1) White, J. M. (1992) Membrane fusion. *Science 258*, 917−924.

(2) Colman, P. M., and Lawrence, M. C. (2003) The structural biology of type I viral membrane fusion. *Nat. Rev. Mol. Cell Biol. 4*, 309−319.

(3) Poranen, M. M., Daugelavicius, R., and Bamford, D. H. (2002) Common principles in viral entry. *Annu. Rev. Microbiol. 56*, 521−538.

(4) Gallo, S. A., Finnegan, C. M., Viard, M., Raviv, Y., Dimitrov, A., Rawat, S. S., Puri, A., Durell, S., and Blumenthal, R. (2003) The HIV Env-mediated fusion reaction. *Biochim. Biophys. Acta 1614*, 36−50.

(5) Eckert, D. M., and Kim, P. S. (2001) Mechanisms of viral membrane fusion and its inhibition. *Annu. Rev. Biochem. 70*, 777−810.

(6) Furuta, R. A., Wild, C. T., Weng, Y., and Weiss, C. D. (1998) Capture of an early fusion-active conformation of HIV-1 gp41. *Nat. Struct. Biol. 5*, 276−279.

(7) Jiang, S., Lin, K., Strick, N., and Neurath, A. R. (1993) HIV-1 inhibition by a peptide. *Nature 365*, 113.

(8) Epand, R. M. (2003) Fusion peptides and the mechanism of viral fusion. *Biochim. Biophys. Acta 1614*, 116−121.

(9) Freed, E. O., Myers, D. J., and Risser, R. (1990) Characterization of the fusion domain of the human immunodeficiency virus type 1 envelope glycoprotein gp41. *Proc. Natl. Acad. Sci. U.S.A. 87*, 4650−4654.

(10) Pritsker, M., Rucker, J., Hoffman, T. L., Doms, R. W., and Shai, Y. (1999) Effect of nonpolar substitutions of the conserved Phe11 in the fusion peptide of HIV-1 gp41 on its function, structure, and organization in membranes. *Biochemistry 38*, 11359−11371.

(11) Chan, D. C., Fass, D., Berger, J. M., and Kim, P. S. (1997) Core structure of gp41 from the HIV envelope glycoprotein. *Cell 89*, 263−273.

(12) Weissenhorn, W., Dessen, A., Harrison, S. C., Skehel, J. J., and Wiley, D. C. (1997) Atomic structure of the ectodomain from HIV-1 gp41. *Nature 387*, 426−430.

(13) Melikyan, G. B., Markosyan, R. M., Hemmati, H., Delmedico, M. K., Lambert, D. M., and Cohen, F. S. (2000) Evidence that the transition of HIV-1 gp41 into a six-helix bundle, not the bundle configuration, induces membrane fusion. *J. Cell Biol. 151*, 413−423.

(14) Munoz-Barroso, I., Durell, S., Sakaguchi, K., Appella, E., and Blumenthal, R. (1998) Dilation of the human immunodeficiency virus-1 envelope glycoprotein fusion pore revealed by the inhibitory action of a synthetic peptide from gp41. *J. Cell Biol. 140*, 315−323.

(15) He, Y., Cheng, J., Li, J., Qi, Z., Lu, H., Dong, M., Jiang, S., and Dai, Q. (2008) Identification of a critical motif for the human immunodeficiency virus type 1 (HIV-1) gp41 core structure: Implications for designing novel anti-HIV fusion inhibitors. *J. Virol. 82*, 6349−6358.

(16) Wexler-Cohen, Y., and Shai, Y. (2007) Demonstrating the C-terminal boundary of the HIV 1 fusion conformation in a dynamic ongoing fusion process and implication for fusion inhibition. *FASEB J. 21*, 3677−3684.

(17) Wexler-Cohen, Y., Ashkenazi, A., Viard, M., Blumenthal, R., and Shai, Y. (2010) Virus-cell and cell-cell fusion mediated by the HIV-1 envelope glycoprotein is inhibited by short gp41 N-terminal membrane-anchored peptides lacking the critical pocket domain. *FASEB J. 24*, 4196−4202.

(18) Reuven, E. M., Dadon, Y., Viard, M., Manukovsky, N., Blumenthal, R., and Shai, Y. (2012) HIV-1 gp41 transmembrane domain interacts with the fusion peptide: Implication in lipid mixing and inhibition of virus-cell fusion. *Biochemistry 51*, 2867−2878.

(19) Noah, E., Biron, Z., Naider, F., Arshava, B., and Anglister, J. (2008) The membrane proximal external region of the HIV-1 envelope glycoprotein gp41 contributes to the stabilization of the six-helix bundle formed with a matching N′ peptide. *Biochemistry 47*, 6782−6792.

(20) Buzon, V., Natrajan, G., Schibli, D., Campelo, F., Kozlov, M. M., and Weissenhorn, W. (2010) Crystal structure of HIV-1 gp41 including both fusion peptide and membrane proximal external regions. *PLoS Pathog. 6*, e1000880.

(21) Caffrey, M. (2001) Model for the structure of the HIV gp41 ectodomain: Insight into the intermolecular interactions of the gp41 loop. *Biochim. Biophys. Acta 1536*, 116−122.

(22) Schulz, T. F., Jameson, B. A., Lopalco, L., Siccardi, A. G., Weiss, R. A., and Moore, J. P. (1992) Conserved structural features in the interaction between retroviral surface and transmembrane glycoproteins? *AIDS Res. Hum. Retroviruses 8*, 1571−1580.

(23) Caffrey, M., Cai, M., Kaufman, J., Stahl, S. J., Wingfield, P. T., Covell, D. G., Gronenborn, A. M., and Clore, G. M. (1998) Three-dimensional solution structure of the 44 kDa ectodomain of SIV gp41. *EMBO J. 17*, 4572−4584.

(24) Merrifield, R. B., Vizioli, L. D., and Boman, H. G. (1982) Synthesis of the antibacterial peptide cecropin A (1−33). *Biochemistry 21*, 5020−5031.
(25) Wexler-Cohen, Y., Johnson, B. T., Puri, A., Blumenthal, R., and Shai, Y. (2006) Structurally altered peptides reveal an important role for N-terminal heptad repeat binding and stability in the inhibitory action of HIV-1 peptide DP178. *J. Biol. Chem. 281*, 9005−9010.
(26) Struck, D. K., Hoekstra, D., and Pagano, R. E. (1981) Use of resonance energy transfer to monitor membrane fusion. *Biochemistry 20*, 4093−4099.
(27) Pascual, R., Moreno, M. R., and Villalain, J. (2005) A peptide pertaining to the loop segment of human immunodeficiency virus gp41 binds and interacts with model biomembranes: Implications for the fusion mechanism. *J. Virol. 79*, 5142−5152.
(28) Poumbourios, P., Maerz, A. L., and Drummer, H. E. (2003) Functional evolution of the HIV-1 envelope glycoprotein 120 association site of glycoprotein 41. *J. Biol. Chem. 278*, 42149−42160.
(29) Jacobs, A., Sen, J., Rong, L., and Caffrey, M. (2005) Alanine scanning mutants of the HIV gp41 loop. *J. Biol. Chem. 280*, 27284−27288.
(30) Gallaher, W. R., Ball, J. M., Garry, R. F., Griffin, M. C., and Montelaro, R. C. (1989) A general model for the transmembrane proteins of HIV and other retroviruses. *AIDS Res. Hum. Retroviruses 5*, 431−440.
(31) Moreno, M. R., Giudici, M., and Villalain, J. (2006) The membranotropic regions of the endo and ecto domains of HIV gp41 envelope glycoprotein. *Biochim. Biophys. Acta 1758*, 111−123.
(32) Peisajovich, S. G., Blank, L., Epand, R. F., Epand, R. M., and Shai, Y. (2003) On the interaction between gp41 and membranes: The immunodominant loop stabilizes gp41 helical hairpin conformation. *J. Mol. Biol. 326*, 1489−1501.
(33) Bar, S., and Alizon, M. (2004) Role of the ectodomain of the gp41 transmembrane envelope protein of human immunodeficiency virus type 1 in late steps of the membrane fusion process. *J. Virol. 78*, 811−820.
(34) Ashkenazi, A., Viard, M., Wexler-Cohen, Y., Blumenthal, R., and Shai, Y. (2011) Viral envelope protein folding and membrane hemifusion are enhanced by the conserved loop region of HIV-1 gp41. *FASEB J. 25*, 2156−2166.
(35) Syu, W. J., Lee, W. R., Du, B., Yu, Q. C., Essex, M., and Lee, T. H. (1991) Role of conserved gp41 cysteine residues in the processing of human immunodeficiency virus envelope precursor and viral infectivity. *J. Virol. 65*, 6349−6352.
(36) Barbouche, R., Miquelis, R., Jones, I. M., and Fenouillet, E. (2003) Protein-disulfide isomerase-mediated reduction of two disulfide bonds of HIV envelope glycoprotein 120 occurs post-CXCR4 binding and is required for fusion. *J. Biol. Chem. 278*, 3131−3136.
(37) Chernomordik, L. V., and Kozlov, M. M. (2005) Membrane hemifusion: Crossing a chasm in two leaps. *Cell 123*, 375−382.